

Doppler-Shifted Acoustic Cyclotron Resonance in Gallium*

J. A. MUNARIN†

Argonne National Laboratory, Argonne, Illinois

(Received 8 February, 1968)

The absorption of 260-MHz longitudinal sound waves in single crystals of gallium has been measured at 1.2° K for propagation along the [100] axis. With the magnetic field in the (001) and (010) planes, sharp resonant peaks in the attenuation are observed over a large angular range centered on the propagation axis. Two series of absorption maxima, degenerate in the (010) plane, are attributed to a magnetoacoustic density-of-states resonance of seventh-band electron orbits for which the differential area dA/dk_z is an extremum. The average drift velocity and cyclotron effective mass obtained from the Doppler splitting are compared with corresponding parameters in the nearly free-electron approximation. Other resonances near the [100] axis are identified with seventh- and eighth-band orbits and are correlated with dc size-effect measurements. A Doppler-shifted open-orbit resonance for $\mathbf{H} \parallel [010]$ associated with the sixth-band hole surface which permits open orbits in the [001] direction is described. The carrier drift along the sound propagation is obtained from the separation of corresponding subharmonic peaks for $\pm n$.

I. INTRODUCTION

THE study of resonant attenuation of ultrasonic waves in the presence of a magnetic field has led to significant advances in our understanding of the Fermi surface (FS) of many of the pure metals and semimetals.¹ In the liquid-helium temperature range, the absorption is primarily due to interaction of the acoustic phonons with conduction electrons and is a periodic function of $|\mathbf{q}|/|\mathbf{H}|$, where \mathbf{q} is the propagation vector and \mathbf{H} the magnetic field. The positions of the attenuation maxima can be related to linear dimensions, the gradient of the orbital area, or Gaussian curvature of the FS at the limiting points, depending upon the direction of \mathbf{q} and the orientation of the magnetic field.

In the normal geometry, $\mathbf{q} \perp \mathbf{H}$, the attenuation is a relative maximum (or minimum) whenever the extremal orbit is exactly calipered by the sound wave, $\mathbf{q} \cdot \mathbf{R} = 2\pi n$, provided that $ql > 1$, where l is the electronic mean free path. The period of the transverse magnetoacoustic effect (geometric resonance) is simply related to the radius of the FS under the appropriate symmetry conditions,² and detailed studies have been useful in mapping the extremal orbits in the principal planes in many cases. If $\mathbf{q} \cdot \mathbf{H} \neq 0$, geometric resonance may still be observed, but the relationship between the harmonic oscillations and the orbital parameters cannot be inverted without a detailed model.³

Of greater interest in the oblique geometry are the sharp resonant peaks and edges due to Doppler-shifted cyclotron resonance of the conduction electrons in the applied magnetic field. These arise from poles in the conductivity (see Sec. II) when the cyclotron frequency

ω_c becomes equal to a submultiple of the effective sound frequency, $\omega_{\text{eff}} = \pm n\omega_c$, and for closed orbits are connected with the electron drift along the magnetic field $|\langle \mathbf{v} \rangle| = \langle v_z \rangle$. In the frame of reference of the moving electron, the frequency of the acoustic disturbance is Doppler shifted to an effective value $\omega_{\text{eff}} = \omega(1 + \hat{q} \cdot \langle \mathbf{v} \rangle / v_s)$, where \hat{q} is the unit propagation vector and v_s is the velocity of sound.⁴ In a typical metal, the ratio $\langle v_z \rangle / v_s$ is about 10^3 which implies that the resonance condition for $H \leq 10$ kOe can be satisfied at frequencies of the order of 100 MHz. Above the limiting field $H_A = (\omega m^* c / e)(v_F / v_s) \cos \theta$, which defines the fundamental absorption edge, where v_F is the limiting-point Fermi velocity and $\cos \theta = \hat{q} \cdot \hat{H}$, the electronic attenuation drops sharply to zero since no electron on the FS can absorb sound resonantly. For $H < H_A$, Eckstein has shown that the attenuation oscillates as the resonant electrons simultaneously come into spatial (geometric) resonance with the sound wave.⁵

When the FS is nonellipsoidal, resonant contributions to the attenuation also come from nonlimiting orbits for which there is a singularity in the density of states with respect to $m^* \langle v_z \rangle$.⁶ The condition is equivalent to $d^2 A / dk_z^2 = 0$, which corresponds to an extremum in the function $dA(k_z, E) / dk_z = -2\pi m^* \langle v_z \rangle / \hbar$. The attenuation peaks are true resonances with Lorentzian line shape and width $\Delta H / H \sim (\omega \tau)^{-1}$, independent of n , where τ is the bulk relaxation time. The density-of-states resonance has been tentatively identified in antimony,⁷ cadmium,⁸ aluminum,⁹ and rhenium,¹⁰ but no systematic

⁴ When $\mathbf{q} \perp \mathbf{H}$, the electron drift for closed orbits has no component in the direction of \mathbf{q} , and hence the acoustic cyclotron resonances are not Doppler shifted. Transverse cyclotron resonances have been observed only in gallium to date, because of the stringent requirement $\omega \tau \gg 1$ (see Sec. II).

⁵ S. G. Eckstein, Phys. Letters **20**, 144 (1966).

⁶ S. G. Eckstein, Phys. Rev. Letters **16**, 611 (1966).

⁷ Y. Eckstein, Phys. Letters **20**, 606 (1966).

⁸ L. Mackinnon, M. T. Taylor, and M. R. Daniel, Phil. Mag. **7**, 523 (1962); L. Mackinnon and M. R. Daniel, Phys. Letters **1**, 157 (1962).

⁹ B. K. Jones, Phil. Mag. **9**, 217 (1964).

¹⁰ L. R. Testardi and R. R. Soden, Phys. Rev. **158**, 581 (1967)

* Based on work performed under the auspices of the U. S. Atomic Energy Commission.

† Present address: Department of Physics, Indiana University, Bloomington, Ind.

¹ A recent review of magnetoacoustic effects in metals has been given by Normal Tepley, Proc. IEEE **53**, 1586 (1965).

² J. B. Ketterson and R. W. Stark, Phys. Rev. **156**, 748 (1967).

³ Y. Eckstein, in *Proceedings of the Tenth International Conference on Low-Temperature Physics, Moscow, 1966* (VINITY, Moscow, 1967).

angular correlation to a model FS has been made in any case.

Previous magnetoacoustic measurements in gallium of the geometric resonance oscillations¹¹ and acoustic cyclotron resonance^{12,13} have been restricted to the normal geometry $\mathbf{q} \perp \mathbf{H}$. In the present work, we have measured the Doppler-shifted cyclotron peaks in the oblique geometry with $\mathbf{q} \parallel [100]$ and H in the (001) and (010) planes for 260 MHz longitudinal propagation. A description of the experimental techniques (Sec. III) follows a brief theoretical discussion in Sec. II. Section IV is devoted to a description of the measurements which are interpreted and compared with theoretical nearly free-electron parameters in Sec. V.

II. THEORY

Magnetoacoustic resonance effects have been studied in detail by Kaner *et al.*¹⁴ for strong deformation-potential coupling of the sound wave to the conduction electrons and by Eckstein^{5,6} when the coupling is electromagnetic. According to Ref. 5, the diagonal elements of the conductivity which appear in the absorption coefficient can be written quite generally in the form

$$\text{Re}\sigma_{ii} = \text{Re} \sum_{n=-\infty}^{\infty} \int \frac{F_n(k_z, H) dk_z}{1 + i(n\omega_c \tau - \mathbf{q} \cdot \langle \mathbf{v} \rangle \tau - \omega \tau)}, \quad (1)$$

in which the Bessel functions, which give rise to the geometric resonance oscillations, are contained in the real function $F_n(k_z, H)$. If the relaxation time τ is large and $\langle v_z \rangle$ is positive, the condition for cyclotron resonance is approximately

$$\mathbf{q} \cdot \langle \mathbf{v} \rangle + \omega = n\omega_c, \quad n = 1, 2, 3, \dots \quad (2)$$

neglecting all nonresonant contributions to the summation over n . Below the absorption edge, the conductivity is proportional to the number of electrons which satisfy Eq. (2) and, hence, the main contribution to the integration over k_z comes from orbits which correspond to a pole in the density of states with respect to $m^* \langle v_z \rangle$. Since $dN/d(m^* \langle v_z \rangle) = (dN/dk_z) / [d(m^* \langle v_z \rangle)/dk_z]$, this is equivalent to $d^2A/dk_z^2 = 0$. The width of the resonance $\Delta\omega_c/\omega_c \sim [\omega\tau(1 + v_z \cos\theta/v_s)]^{-1}$ is of order $10^{-3}(\omega\tau)^{-1}$ except when \mathbf{H} is very nearly perpendicular to \mathbf{q} , in which case $\Delta\omega_c/\omega_c \sim (\omega\tau)^{-1}$. When $q\langle v_z \rangle \tau \cos\theta \gg 1$, the field at which the extremal orbit comes into resonance with the sound wave depends on the sign of $\mathbf{q} \cdot \langle \mathbf{v} \rangle$.

From Eq. (2)

$$H_{n\pm} = \frac{\omega m^* c}{ne} \left(\frac{\langle v_z \rangle}{v_s} \cos\theta \pm 1 \right) \quad (3)$$

for propagation parallel (−) or antiparallel (+) to the electron drift. Solving for m^* and $\langle v_z \rangle$,

$$m^* = (ne/2\omega c)(H_{n+} - H_{n-}),$$

$$\langle v_z \rangle = \frac{v_s}{\cos\theta} \left(\frac{H_{n+} + H_{n-}}{H_{n+} - H_{n-}} \right). \quad (4)$$

In the transverse case $\mathbf{q} \cdot \mathbf{H} = 0$, Doppler-shifted cyclotron resonance is only possible when the FS is open, in which case the drift of the electrons in the magnetic field again has a component $\langle v_x \rangle$ in the propagation direction. With the same approximations as before, the condition for open-orbit resonance is

$$(1 + \langle v_x \rangle / v_s) \omega T = 2\pi n, \quad n = \pm 1, \pm 2, \dots \quad (5)$$

where T is the period of the open orbit. The position of the resonance depends on the repeat distance k_0 along the orbit as well as the drift velocity

$$H_{n\pm} = \frac{qch k_0}{2\pi |n| e} (1 \pm v_s / \langle v_x \rangle), \quad (6)$$

which leads to

$$k_0 = (\pi ne / qch) (H_{n+} + H_{n-}),$$

$$\langle v_x \rangle = v_s \left(\frac{H_{n+} + H_{n-}}{H_{n+} - H_{n-}} \right), \quad (7)$$

for $q\langle v_x \rangle \tau \gg 1$.

The resonance conditions Eqs. (2) and (5) can also be obtained from the conservation of energy and momentum in the electron-phonon interaction, in which case the number of n appears as the difference in initial and final Landau levels of the conduction electrons quantized by the magnetic field. Kotkin¹⁵ has shown that the selection rule for the absorption of longitudinal phonons is $n = rs$, where r is an integer and the relevant sheet of the FS is s -fold symmetric. The period of the resonant oscillations obtained from Eq. (3) is

$$\Delta \left(\frac{1}{H} \right) = \frac{es}{qm^* c \langle v_z \rangle \cos\theta}. \quad (8)$$

III. EXPERIMENTAL DETAILS

Single crystals of the required orientation for acoustic propagation along the [100] axis were obtained by seeded growth from the melt¹⁶ from material with less than 1-ppm impurity content. The Plexiglas mold,

¹¹ P. A. Bezuglyi, A. A. Galkin, and S. E. Zhevago, Zh. Eksperim. i Teor. Fiz. **47**, 825 (1964) [English transl.: Soviet Phys.—JETP **20**, 552 (1965)].

¹² B. W. Roberts, Phys. Rev. Letters **6**, 453 (1961).

¹³ Jacques Lewiner, Phys. Rev. Letters **19**, 1037 (1967).

¹⁴ E. A. Kaner, Zh. Eksperim. i Teor. Fiz. **38**, 212 (1960) [English transl.: Soviet Phys.—JETP **11**, 154 (1960)]; E. A. Kaner, V. G. Peschanskii, and I. A. Privorotskii, *ibid.* **40**, 214 (1961) [English transl.: *ibid.* **13**, 147 (1961)]; E. A. Kaner, *ibid.* **43**, 216 (1962) [English transl.: *ibid.* **16**, 154 (1963)].

¹⁵ G. I. Kotkin, Zh. Eksperim. i Teor. Fiz. **41**, 281 (1961) [English transl.: Soviet Phys.—JETP **14**, 210 (1962)].

¹⁶ Yu. V. Sharvin and V. F. Gantmakher, Priboiy i Tekhnika Eksperimenta **6**, 165 (1963) [English transl.: Instr. Exper. Tech. **6**, 1169 (1963)].

which was spring loaded to allow for expansion of the solid phase ($\sim 3\%$), included end plates which had been ground flat and polished. Access to the cylindrical cavity, $\frac{3}{8}$ in. in diam and $\frac{1}{2}$ in. long, was through four $\frac{1}{16}$ -in. channels, one of which was drilled to accommodate a syringe used to fill the mold. The three overflow channels were fitted with simple conical relief valves made of teflon to allow the excess liquid to escape. Before assembly, the internal surfaces of the mold were given a light coating of silicone oil to facilitate removal of the crystal. The seed, mounted on a goniometer head and previously aligned with the axis of the mold by x-ray diffraction, was brought into contact with the liquid column protruding from the filling channel. The low melting point (29.8°C) and long supercooling range allowed the preparation of the crystal to be carried out at room temperature. The four arms extending from the lateral surface of the sample were removed by spark erosion, but damage to the active volume of the sample was minimal since the transducer area was only $\frac{1}{4}$ in. in diam and no further preparation of the end faces was necessary.

The quartz transducers with 20-MHz fundamental frequency, used for longitudinal propagation, were bonded to the samples with Dow Corning silicone oil of 20 000-centistoke viscosity. The specimen holder allowed propagation in the plane of rotation of the magnetic field so that any plane parallel to the wavevector \mathbf{q} could be measured simply by rotating the sample within its mount.

Regulated magnetic fields within the range 0–10 kOe were provided by a Harvey Wells 12-in. watercooled magnet with control circuitry designed to give linear and inverse time sweeps.¹⁷ The magnetic field readout was obtained from a Bell BH-701 Hall probe operating with 100-mA control current. The linearity in field was better than $\frac{1}{4}\%$ and the calibration was set at several points by NMR.

Pulse-echo measurements of the ultrasonic attenuation were made primarily at 260 MHz with a repetition rate of 100 Hz. The system, described in detail elsewhere,¹⁸ utilized a pulsed-cavity oscillator to provide up to 1 kW rf power to the transmitting transducer bonded to the sample. The echo pulse was detected and then gated and integrated and recorded directly as a function of magnetic field. Stub tuners were occasionally used to improve the impedance match between the sample and transmitter and receiver.

The velocity of sound for longitudinal propagation along the [100] axis, measured by the pulse-echo technique at 60 MHz, was found to be 4.24×10^5 cm/sec at 1.2°K in good agreement with the value 4.17×10^5 cm/sec obtained in Ref. 11 at liquid-hydrogen temperature. The sample length was corrected for thermal

contraction according to the lattice parameters determined by Barrett¹⁹ from x-ray diffraction.

IV. EXPERIMENTAL RESULTS

Measurements of the absorption of 260-MHz compressional waves in a magnetic field were made in the (001) and (010) planes on three single crystals whose axes were aligned with the crystallographic [100] direction to within 1° .²⁰ At this frequency, the sound attenuation $\Gamma(H)$ was strongly field dependent in the range 0–10 kOe, exhibiting resonant oscillations characteristic of Doppler-shifted cyclotron resonance as well as harmonic oscillations due to geometric resonance for $\hat{H} \cdot \hat{q} \sim 0$ and quantum oscillations independent of ω for $H > 4$ kOe. Due to the exceptionally long relaxation time τ and to the specific form of the FS, the resonant maxima were extremely well defined and persisted for very large values of $\theta = \cos^{-1}(\hat{q} \cdot \hat{H})$, thus prompting the following investigation. The attenuation $\Gamma(H)$ is plotted as a function of H in Figs. 1–6.

In the parallel field case, $\mathbf{H} \parallel \mathbf{q}$, the attenuation, shown in Fig. 1, exhibits a large number of resonant peaks, roughly periodic in $1/H$, which fall into four distinct series with periods ranging from 0.100×10^{-3} Oe $^{-1}$ to 0.569×10^{-3} Oe $^{-1}$ (see Table I). The linewidth ΔH indicates that the mean free path l is greater than 1 cm,²¹ consistent with the estimate given by Roberts¹² for acoustic propagation along the [001] axis. At the operating frequency, 260 MHz, this implies that ql is about 3500 and ql_z is approximately 100, so that the condition for geometric resonance, $ql > 1$, as well as the required $ql_z > 1$ necessary for Doppler-shifted cyclotron resonance, is well satisfied. The Doppler splitting ($H_{n+} - H_{n-}$) is a measure of $m^*\omega$, where m^* is the effective cyclotron mass, whereas the mean position of the upper and lower resonance, $\frac{1}{2}(H_{n+} + H_{n-})$, is directly related to the product $m^*\langle v_z \rangle$ so that m^* and $\langle v_z \rangle$ can be determined independently. The inverse relation between the linewidth and sound frequency (Sec. II) was verified by measuring $\Gamma(H)$ at 466 MHz with $\hat{H} \parallel \hat{q}$.

At low fields, the attenuation is dominated by the α resonance with fundamental at 1.77 kOe. The velocity $\langle v_z \rangle = 3.22 \times 10^7$ cm/sec is about one-sixth the Fermi velocity, v_F , and m^* is $0.25m_0$, where m_0 is the electron rest mass. The α oscillations for $\hat{H} \parallel \hat{q}$ were first noted by Bezuglyi, Galkin, and Zhevago²² but their value of $\omega\tau$ did not resolve the Doppler splitting so that only the product $m^*\langle v_z \rangle = 7.4 \times 10^{-21}$ g cm/sec could be determined. The present results for $\mathbf{H} \parallel \mathbf{q} \parallel [100]$ are in good

¹⁹ Quoted in J. C. Slater, G. F. Koster, and J. H. Wood, Phys. Rev. **126**, 1307 (1962).

²⁰ A preliminary report on this work appeared in Bull. Am. Phys. Soc. **12**, 332 (1967).

²¹ $l = v_F\tau \sim 2\hbar k_F c / ne\Delta H$.

²² P. A. Bezuglyi, A. A. Galkin, and S. E. Zhevago, Fiz. Tverd. Tela **7**, 480 (1965) [English transl.: Soviet Phys.—Solid State **7**, 383 (1965)].

¹⁷ J. B. Ketterson and Y. Eckstein, Rev. Sci. Instr. **37**, 44 (1966).

¹⁸ J. B. Ketterson and Y. Eckstein, Phys. Rev. **140**, A1355 (1965).

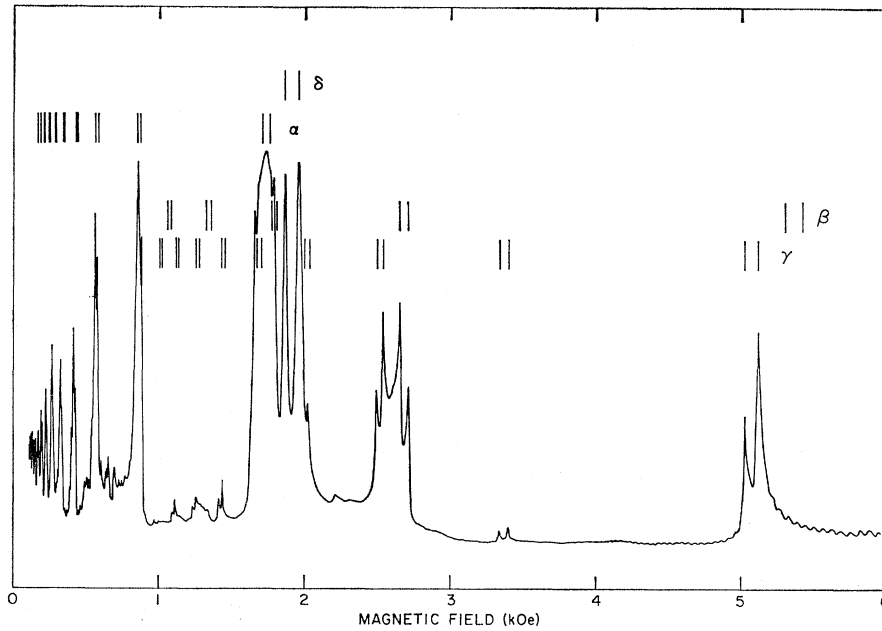


FIG. 1. Attenuation of 260-MHz compressional waves in the longitudinal configuration $\mathbf{H} \parallel \mathbf{q} \parallel [100]$. Doppler-shifted cyclotron-resonance maxima corresponding to periods α , β , γ , and δ are indicated by reference markings above the curve. The fundamental α resonance is clipped because the pulse height extends into the noise background.

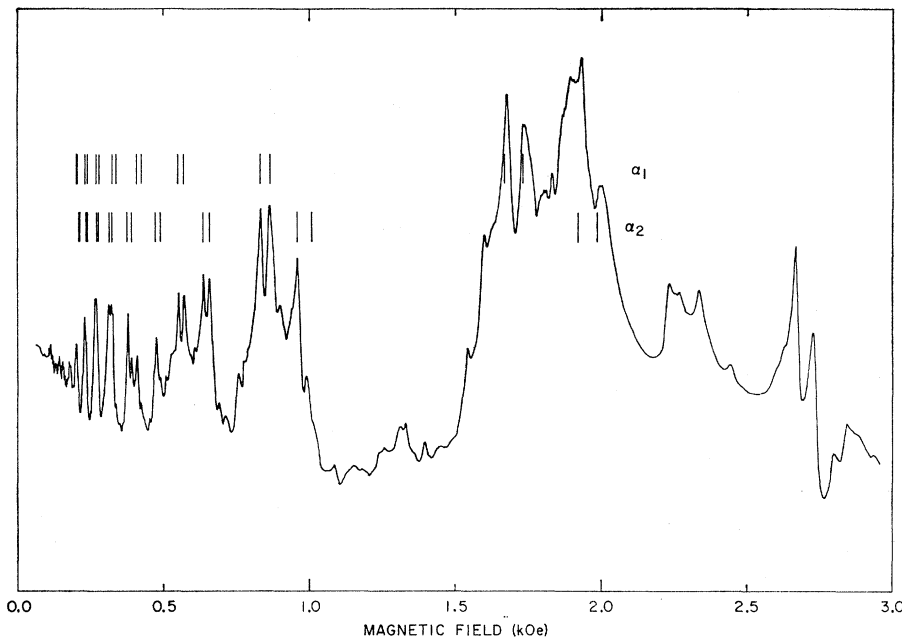


FIG. 2. Splitting of the α resonance in the (001) plane, $\theta = 5^\circ$, where $\theta = \cos^{-1}(\hat{q} \cdot \hat{H})$.

agreement, but extend the measurements to the oblique geometry $\hat{q} \cdot \hat{H} < 1$.

The β resonance in Fig. 1 has basic period $0.188 \times 10^{-3} \text{ Oe}^{-1}$, corresponding to the dominant magneto-resistance size-effect oscillations for $\mathbf{H} \parallel [100]$ with $dA/dk_z = 1.322 \times 10^8 \text{ cm}^{-1}$.²³ This period arises from extremal body orbits on the L -centered butterfly in the seventh band, closely associated with the similarly

located cigar in the eighth band. According to the selection rules given by Kotkin¹⁵ for longitudinal waves, the twofold symmetry of these orbits accounts for the low amplitude of the fundamental resonance and strong second subharmonic ($n=2$) at 2.680 kOe. These oscillations yield $m^* = 0.65m_0$ and drift velocity $\langle v_z \rangle = 3.77 \times 10^7 \text{ cm/sec}$.

The third set of resonant oscillations γ with period $0.100 \times 10^{-3} \text{ Oe}^{-1}$ approximately $\frac{1}{2} \Delta(1/H)_\beta$ is characterized by large-amplitude second and fourth sub-

²³ J. A. Munarin, J. A. Marcus, and P. E. Bloomfield, Phys. Rev. 172, 718 (1968).

FIG. 3. The α_1 resonance for $\theta=65^\circ$ in the (001) plane.

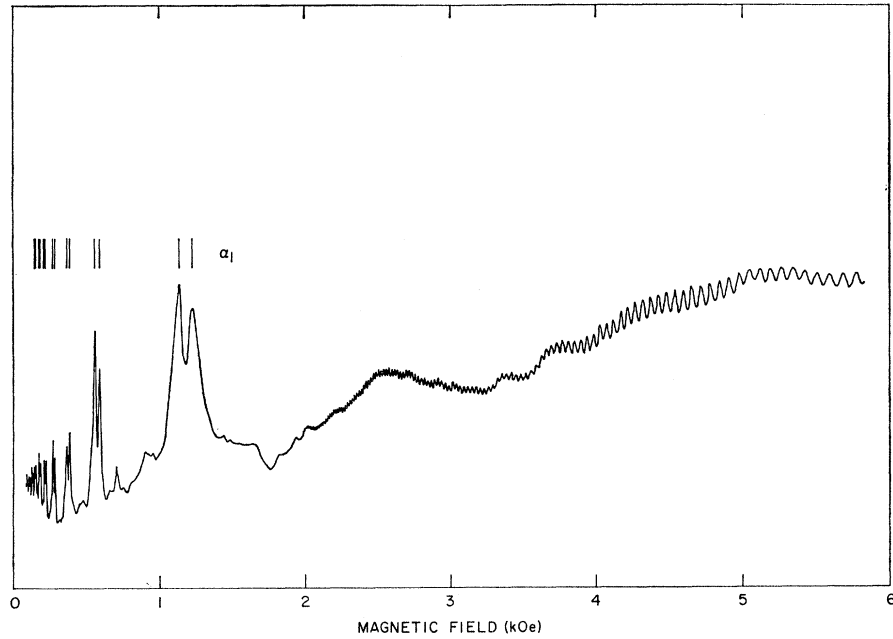
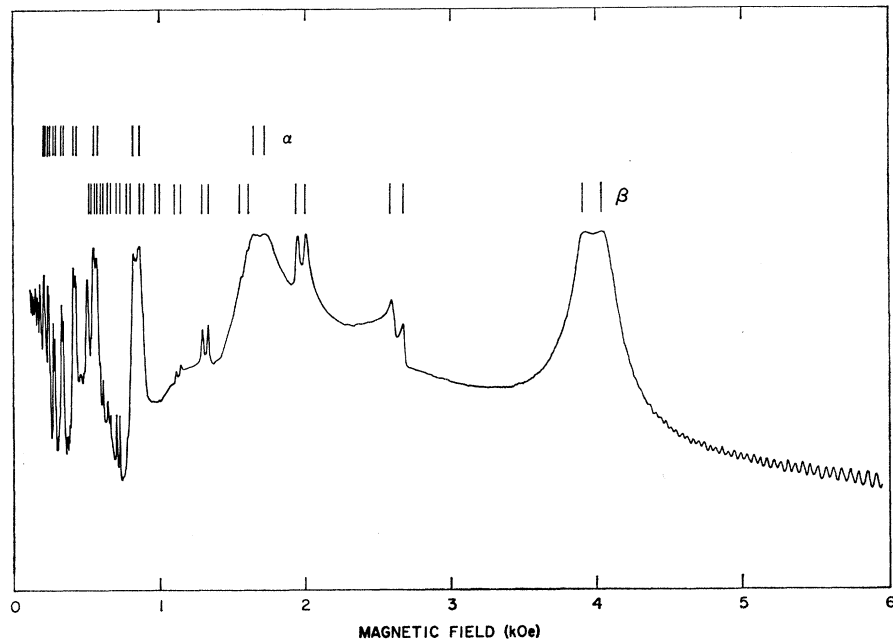


FIG. 4. Resonant oscillations in the attenuation for $q \parallel [100]$ and $\theta=30^\circ$ in the (010) plane, $\theta = \cos^{-1}(\hat{q} \cdot \hat{H})$. The fundamental α resonance and $n=2$ β resonance are limited by the noise background.



harmonics at 5.075 and 2.515 kOe, respectively, and weak but measurable third subharmonic resonance at 3.365 kOe with amplitude down by a factor of 20. The corresponding extremal orbits (see Sec. V) with mass $0.94m_0$ and $\langle v_z \rangle = 4.90 \times 10^7$ cm/sec are nearly twofold symmetric about the field direction and are probably closely related to the β orbits.

The sharp resonance lines at 1.860 and 1.955 kOe (δ) appear to be unrelated to other peaks in $\Gamma(H)$ in Fig. 1, but detailed measurement shows that a low-amplitude second harmonic is present at 0.902 kOe, from which

the period $\Delta(1/H)_\delta = 0.526 \times 10^{-8} \text{ Oe}^{-1}$ is obtained. From the fundamental resonance which is well resolved, the effective carriers have $\langle v_z \rangle = 1.60 \times 10^7$ cm/sec with mass $m^* = 0.54m_0$. The results for $\mathbf{H} \parallel [100]$ are summarized in Table II.

When the field is tilted away from the symmetry axis $[100]$ towards the $[010]$ direction, the α resonance separates into lower and upper branches, α_1 and α_2 (see Fig. 2). The short-period branch α_2 descends quite rapidly with θ (see Fig. 7) and vanishes at approximately 30° from the axis. The upper branch α_1 , on the

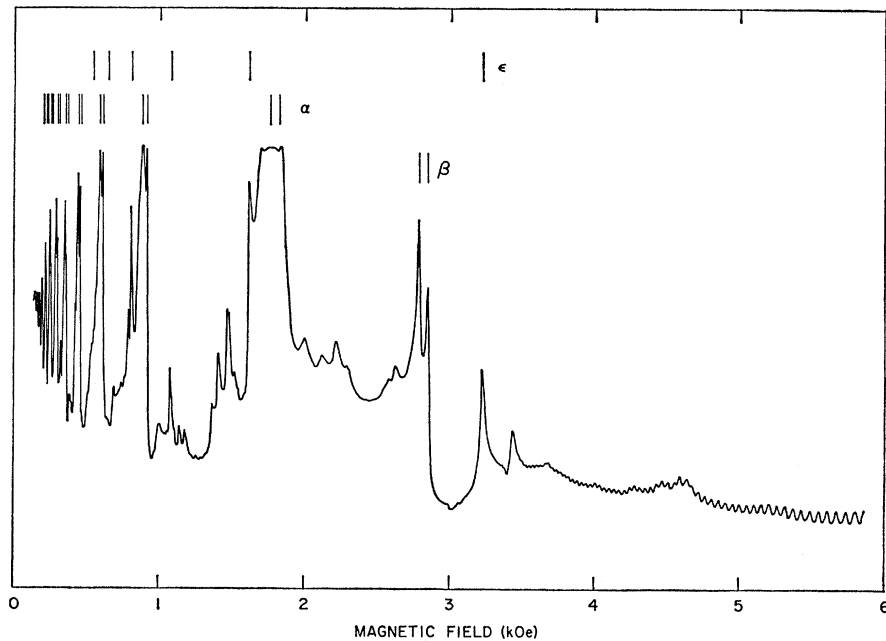


FIG. 5. Field dependence of the attenuation for $\theta=4^\circ$ in the (010) plane showing the ϵ resonant oscillations.

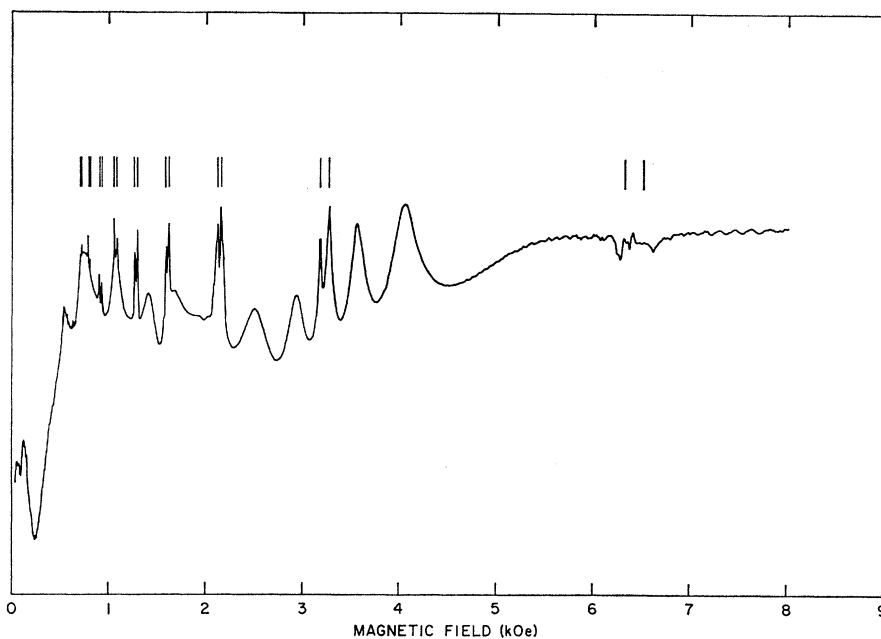


FIG. 6. Open orbit resonance for $q \parallel [100]$ and $H \parallel [010]$. The unusual shape and low amplitude of the fundamental resonance are discussed in the text.

other hand, strongly affects the attenuation over a considerably broader range of θ , extending almost to the $[010]$ axis. The resonance peaks at 65° in Fig. 3 ride upon a background of low-amplitude geometric and quantum oscillations but are still well defined. The plot of period versus θ is S-shaped with minimum curvature at approximately 45° . The β , γ , and δ oscillations are rather insensitive to orientation changes as seen from Fig. 7 and are not well defined for values of θ greater than a few degrees.

In the (010) plane (see Fig. 8) the degeneracy of α_1

and α_2 is not lifted by tilting the field away from the $[100]$ direction, indicating that the extremal orbits are located in separate regions of the FS, either on distinct but similar sheets, or on a single surface, in either case related by mirror symmetry across the (010) plane. The β oscillations are only weakly θ -dependent, but are well developed out to 35° . The period is maximal at 0° with subsidiary minima at $\pm 20^\circ$. The attenuation for 30° in Fig. 4 shows that the β oscillations contain an unusually large harmonic content, which indicates, according to Ref. 15, that the extremal orbit is highly

TABLE I. Doppler-shifted cyclotron resonance ($\mathbf{H} \parallel \mathbf{q} \parallel [100]$).

Period	Subharmonic n	$H_{av} = \frac{1}{2}(H_{n+} + H_{n-})$ (kOe)	$H_{n+} - H_{n-}$ (kOe)
γ	2	5.075	0.090
γ	3	3.365	0.060
β	2	2.680	0.060
γ	4	2.515	0.045
γ	5	2.020	...
δ	1	1.908	0.095
β	3	1.780	...
α	1	1.770	...
γ	6	1.663	0.025
γ	7	1.423	0.025
β	4	1.325	...
γ	8	1.245	0.020
γ	9	1.103	0.015
δ	2	0.902	0.053
α	2	0.894	0.019
α	3	0.596	0.017
α	4	0.445	0.011
α	5	0.354	0.010
α	6	0.293	0.008
α	7	0.248	...
α	8	0.217	...
α	9	0.193	...
α	10	0.173	...

convoluted. This period was observed in the size-dependent magnetoresistance oscillations which are periodic directly in H with frequency $F = ed/2\pi m^* \langle v_z \rangle c \cos\theta$, where d is the thickness of the sample.²³ Since $\Delta(1/H) = e\lambda/2\pi m^* \langle v_z \rangle c \cos\theta$ for the magnetoacoustic resonance, we have $(\Delta H)(\Delta(1/H)) = \lambda/d$, where $\Delta H = 1/F(H)$ is

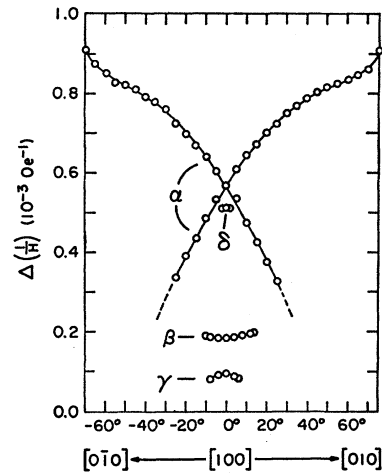
TABLE II. Experimental parameters for $\mathbf{H} \parallel \mathbf{q} \parallel [100]$.

Period	$\Delta(1/H)$ (10^{-3} Oe $^{-1}$)	m^*/m_0	$\langle v_z \rangle$ (10^7 cm/sec)	$(dA/dk_z)_{exp}$ (10^8 cm $^{-1}$)	$(dA/dk_z)_{calc}$ (10^8 cm $^{-1}$)
α	0.569	0.25	3.22	0.436	0.499
β	0.188	0.65	3.77	1.322	1.068
γ	0.100	0.94	4.90	2.485	2.136
δ	0.526	0.54	1.60	0.472	0.365

the period of the size effect. The agreement is within the experimental error wherever the results are available for comparison. The ϵ resonance, not observed in the (001) plane, appears within the range 5° to 25° in the (010) plane (see Fig. 5). The period is strongly angle-dependent, rising sharply in an S-shaped curve from 0.3 to 0.8 kOe $^{-1}$ within 10° .

TABLE III. Open-orbit resonance ($\mathbf{H} \parallel [010]$).

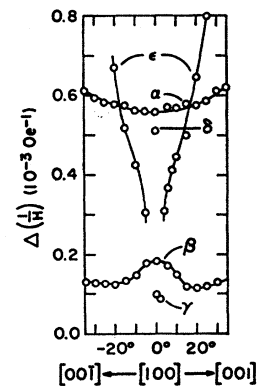
n	$H_{n+} - H_{n-}$ (kOe)	$H_{av} = \frac{1}{2}(H_{n+} + H_{n-})$ (kOe)	H_{av} (predicted) (kOe)
1			6.646
2	0.095	3.228	3.323
3	0.030	2.135	2.215
4	0.025	1.598	1.661
5	0.025	1.283	1.329
6	0.030	1.065	1.108
7	0.020	0.910	0.949
8	0.020	0.795	0.831
9	0.020	0.710	0.738

FIG. 7. Resonance periods in the (001) plane with $\mathbf{q} \parallel [100]$.

With \mathbf{H} aligned with the $[010]$ axis to within 1° , it was possible to observe a sharp resonance shown in Fig. 6 due to open trajectories on the Fermi surface.²⁴ These resonances are of the type described by Galkin, Kaner, and Korolyuk²⁵ in tin but are split due to the large value of $\omega\tau$. The subharmonic resonances are approximately periodic in $1/H$ with period $\Delta(1/H) = 0.155 \times 10^{-3}$ Oe $^{-1}$. From the position of the resonant maxima, given in Table III, the repeat distance along the open orbit k_0 is 1.60×10^8 cm $^{-1}$ which is within 3% of the Brillouin zone size measured in the $[001]$ direction according to the x-ray diffraction data of Barrett.¹⁹ The average drift velocity in the open-orbit direction $\langle v_x \rangle$ is 0.32×10^8 cm/sec, roughly one-sixth the free-electron Fermi velocity $v_F = \hbar k_F/m^*$.

V. DISCUSSION

The Fermi surface of gallium has been subjected to rather extensive investigation through measurements of

FIG. 8. Resonance periods in the (010) plane with $\mathbf{q} \parallel [100]$.

²⁴ J. A. Munarin and Y. Eckstein, Phys. Rev. Letters 19, 1426 (1967).

²⁵ A. A. Galkin, E. A. Kaner, and A. P. Korolyuk, Zh. Eksperim. i Teor. Fiz. 39, 1517 (1960) [English transl.: Soviet Phys.—JETP 12, 1055 (1961)].

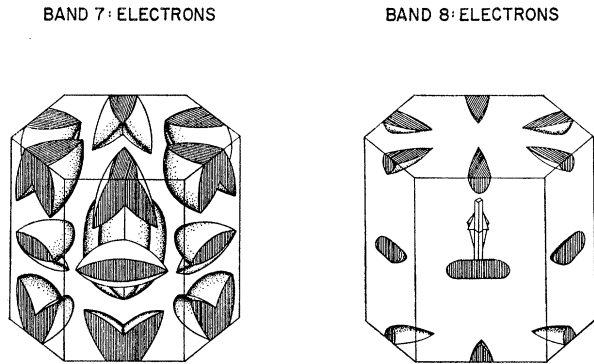


FIG. 11. Band-seven and band-eight electron surface for gallium in the nearly free-electron approximation. The seventh band surface consists of "butterflies" located at the lateral faces of the zone and a star-shaped inner surface at Γ . The band-eight pockets resemble "cigars" located at the same points as the butterflies and a small ribbed surface at Γ .

supports body orbits (a) inside the saddle point as well as lobe orbits (b) with H in the (001) plane. The derivative is maximal at $k_z = 0.04 \text{ \AA}^{-1}$ and has minima at 0.28 and 0.40 \AA^{-1} on the lobes. When H lies in the (010) plane, the lobe extremals are degenerate, which suggest that they are associated with the α resonance. Figure 14 confirms this identification by comparing the average resonant period of the oscillations with the value calculated from the NFE L -centered butterfly in the two measuring planes (001) and (010). In the (001) plane, the periods cross at the [100] axis, although some 10% higher than predicted. The upper branch, corresponding to α_1 , intersects the theoretical curve at 51° while the lower, α_2 , descends rapidly at almost precisely the required rate. In the (010) plane,

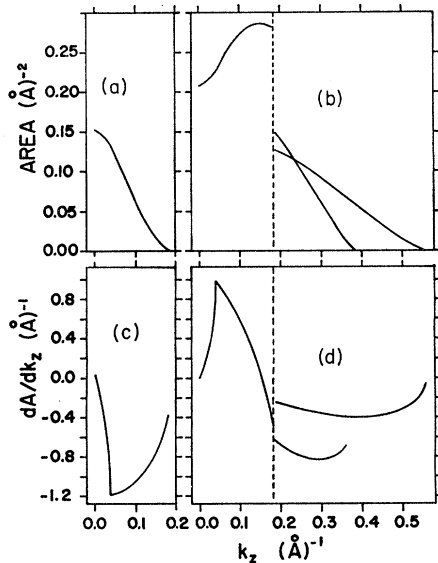


FIG. 12. The orbital area and derivative dA/dk_z for the L -centered butterfly and cigar in the (001) plane, $\theta = 20^\circ$. (a) and (c): cigar; (b) and (d): butterfly.

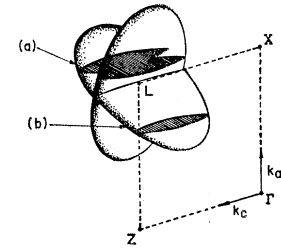


FIG. 13. L -centered butterfly in band seven showing (a) body orbits and (b) lobe orbits.

the predicted extremals remain degenerate for arbitrary θ due to the mirror symmetry of the Fermi surface about the [010] axis and exhibit somewhat stronger angular dependence than the experimental curve. For $H \parallel [100]$, the experimental value of dA/dk_z for the extremal orbit, 0.436 \AA^{-1} , lies within 15% of the value calculated from the NFE model, indicated in Table II. Since differential properties such as $(dA/dk_z)_{\text{extr}}$ are more sensitive to small distortions in the Fermi surface than, say, the extremal area which would be relevant to measurements of the de Haas-van Alphen effect, this agreement is satisfactory. The extremal orbits lie very close to the tip of the butterfly in a region influenced strongly by the Bragg reflection across the (120) plane. The structure factor associated with this reflection vanishes, which means that the band gap is zero in first order.

The effective mass, plotted in Fig. 15, seems to agree in a qualitative way with the NFE model although numerical agreement is as poor as 50%. Similar mass behavior, observed by Moore³⁰ and by Lewiner¹³ in cyclotron resonance, may also be associated with the butterfly although the same extremal orbits are probably not involved.

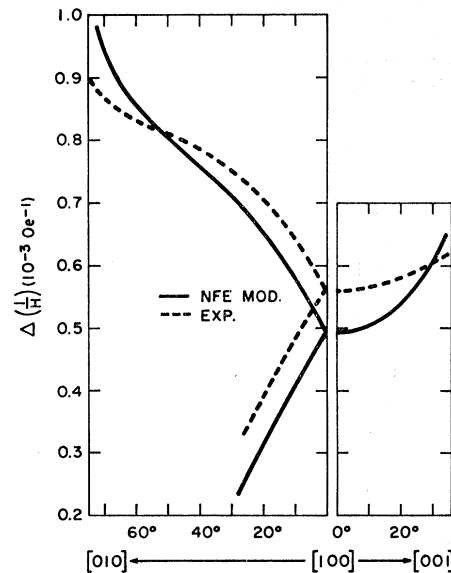


FIG. 14. Comparison of experimental and theoretical α resonance period in (001) and (010) planes.

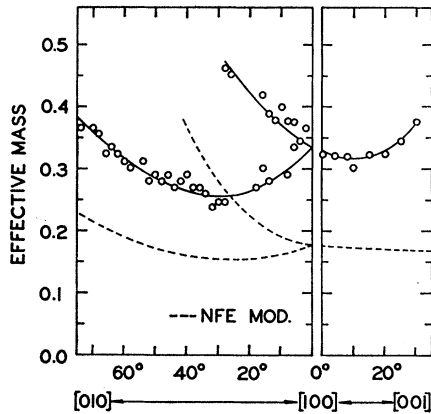


FIG. 15. Cyclotron effective mass associated with α resonance orbits in the (001) and (010) planes.

The period β , identified from size-effect measurements, is probably a composite term and corresponds roughly ($\sim 20\%$) to the minima near the equatorial plane in bands 7 and 8 in Fig. 12. Although the present measurements do not extend over a sufficient range of angle in the (001) plane to establish a definite correspondence with the model Fermi surface, the size-effect frequency data follows very closely the functional dependence calculated for the eighth-band extremal in the ab plane.²³ In this case the strong correlation arises from the zero value of the structure factor for the (100) plane that forms the hexagonal face of the zone. Koster²² has shown that the degeneracy is lifted, however, by spin-orbit effects at all points on this face except along the line XRL in Fig. 9. Therefore, the butterfly and the cigar orbits make contact at only two points, and the situation, taking into account spin-orbit coupling, is as indicated in Fig. 16, which shows (schematically) the extremal orbits for $\mathbf{H}||[100]$. The de Haas-van Alphen measurements of Goldstein and Foner indicate magnetic breakdown across the (100) face of the Brillouin zone and it seems likely that at low fields, breakdown would occur principally on the line XRL . In this case, conditions for magnetic breakdown would be most favorable with the field oriented near the $[100]$ axis, and the period γ may be evidence that this supposition is correct. $\Delta(1/H)_\gamma$ is nearly one-half the β period, corresponding to a single traverse of the electron about the butterfly and the cigar. Equation (2) becomes, approximately, $\mathbf{q} \cdot \langle \mathbf{v} \rangle + \omega = \frac{1}{2} n \omega_c$, which gives resonance oscillation with nearly one-half the basic period. The sum period has also been observed in the size-effect measurements for θ approximately 0° in the (001) plane.

The open-orbit resonance observed for $\mathbf{H}||[010]$ is also suggestive of magnetic breakdown at relatively low fields. According to Reed and Marcus,²⁶ only the zone-6 FS (see Fig. 10) supports open trajectories parallel to the $[001]$ direction in the nearly free-electron model with \mathbf{H} in the (001) plane. These orbits, for $\mathbf{H}||[010]$, shown in Fig. 17, cross the Brillouin-zone boundary at the points P in a noncentral plane and are strongly convoluted, as expected from the large number of sub-

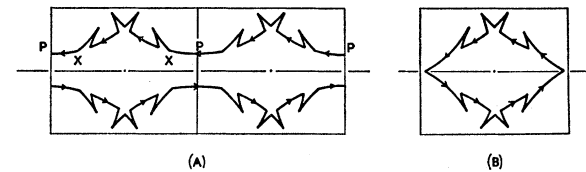


FIG. 17. Open trajectories supported by the band-six hole surface in the nearly-free-electron approximation for $\mathbf{H}||[100]$, (A), and closed breakdown orbit, (B).

harmonics. The unusually low amplitude and shape of the fundamental resonance at approximately 6.4 kOe may indicate that the open trajectory breaks down in closed orbit (B) shown in Fig. 17. The structure factor associated with Bragg reflection at the points X across the (011) plane is identically zero so that the energy gap is zero in first order. If the fundamental resonance is assumed to lie above the breakdown field, the (hole) carrier may follow the free-electron sphere across the Bragg plane along the zone-5 surface, in which case resonant absorption would not be possible. This question can be resolved by measurements at lower acoustic frequencies, which would shift the fundamental resonance line down into the region below the breakdown field.

ACKNOWLEDGMENTS

The author is indebted to Y. Eckstein, S. G. Eckstein, and J. B. Ketterson for helpful discussions, and to the Solid State Science Division of the Argonne National Laboratory for its support of this research.

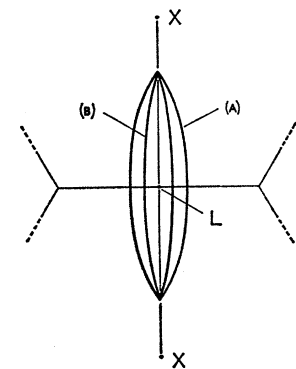


FIG. 16. Butterfly and cigar cross section in the plane of the (100) zone face (schematic). Contact between the band-seven surface (A) and the band-eight surface (B) is maintained along the line XL .

²² G. F. Koster, Phys. Rev. **126**, 2044 (1962).